Vol 14 No 10, October 2005
1009-1963/2005/14(10)/2046-06

Chinese Physics

Numerical simulation for separation of multi-phase immiscible fluids in porous media*

Wu Bai-Zhi(吴柏志)[a)†], Xu You-Sheng(许友生)[b)c)],
Liu Yang(刘 扬)[d)], and Huang Guo-Xiang(黄国翔)[c)]

[a)] *College of Petroleum Engineering, University of Petroleum, Dongying 257061, China*
[b)] *Department of Physics, East China Normal University, Shanghai 200062, China*
[c)] *Department of Physics, Zhejiang Normal University, Jinhua 321004, China*
[d)] *Department of Mechanical Engineering, The Hongkong Polytechnic University, Hong Kong, China*

(Received 11 December 2004; revised manuscript received 16 June 2005)

Based on a lattice Boltzmann method and general principles of porous flow, a numerical technique is presented for analysing the separation of multi-phase immiscible fluids in porous media. The total body force acting on fluid particles is modified by adding relative permeability in Nithiarasu's expression with an additional surface tension term. As a test of this model, we simulate the phase separation for the case of two immiscible fluids. The numerical results show that the two coupling relative permeability coefficients K_{12} and K_{21} have the same magnitude, so the linear flux-forcing relationships satisfy Onsager reciprocity. Phase separation phenomenon is shown with the time evolution of density distribution and bears a strong similarity to the results obtained from other numerical models and the flows in sands. At the same time, the dynamical rules in this model are local, therefore it can be run on massively parallel computers with well computational efficiency.

Keywords: separation of multi-phase immiscible fluids, porous media, numerical simulation
PACC: 4755M, 0340

1. Introduction

In the past several decades, the separation of multi-phase fluids (MPFs) in porous media has attracted considerable attention due to its important applications in geothermal energy systems, secondary and tertiary oil recovery, prevention of subsoil water pollution, and other related fields. The separation of MPFs exhibits a rich variety of pattern formation, including fractal and self-affine growth morphology.[1] Such diverse behaviours are the consequence of growth mechanisms that depend on fluid properties (such as viscosity and surface tension), structures of porous media, and external driving forces that drive the fluids.[2] The separation phenomenon of MPFs in porous media is usually observed at various scales: microscopic scale (pore), macroscopic scale (laboratory, local), and domain scale, etc.[3] Here, the macroscopic scale is defined as a representative element,[4] and it is much larger than the microscopic scale but much smaller than the domain scale. In many situations two or multiple scales may coexist.

The MPFs in porous media are usually investigated by using classical models which can be reduced to the Navier-Stokes equations for porosity equal to 1 or to the earlier porous medium models in appropriate parameter ranges.[5] However, the MPFs in porous media require a more sophisticated description than that provided by a single-phase continuum approach. Many physical properties, such as the relationship between the macroscopic transport coefficients of porous media and their microscopic geometry,[6] the geometrical properties of interfaces,[7] and the relationship between transport coefficients and the morphology of flow, etc, should be considered carefully.[8] Although several different approaches have been introduced, including x-ray microtomography techniques,[9] Laplace transition method,[10] and lattice gas method,[11] etc,

*Project supported by the National Natural Science Foundation of China (Grant No 10302018), the Research Grants Council of the Government of the HKSAR, China (Grant No PolyU5172/020), and the Natural Science Foundation of Zhejiang Province, China (Grant No M103082).
†E-mail: wbz@slof.com

and can provide many improved results, they meet with some problems such as computational efficiency, noise brought by their Boolean nature, non-Galilean invariance, and so on. In recent years, a new method, the lattice Boltzmann method (LBM), has been successfully set up for fluid flows in porous media[2−4,12] and proved powerful, due to its simple implementation, straightforward parallelism, easy grid generation and the capability in simulating MPFs with a complex geometry.

In this paper, we report a comprehensive study on the separation of MPF in a porous medium by combining the LBM with the general principles of porous flow. As a test of our model, we give an example for the case of two immiscible fluids. The paper is organized as follows. In Sec. 2, a model of MPFs in porous media is introduced and a LBM simulation frame for the separation of multi-phase immiscible fluids is described. Section 3 is devoted to the analysis of boundary conditions. In the last section we provide the calculated results of the separation of MPF in a porous medium and give a discussion and summary of our work.

2. The model and lattice-Boltzmann method

We first give a simple description for a MPF flow in a porous medium. We take the form proposed by Nithiarasu *et al.*[5] In this model, the velocity fields $\boldsymbol{v}$ for a single-phase fluid are the solutions of the Navier–Stokes equation

$$\nabla \cdot \boldsymbol{v} = 0, \tag{1}$$

$$\frac{\partial \boldsymbol{v}}{\partial t} + (\boldsymbol{v} \cdot \nabla)\left(\frac{\boldsymbol{v}}{\phi}\right) = -\frac{1}{\rho}\nabla(\phi P) + \nu_e \nabla^2 \boldsymbol{v} + \boldsymbol{F}, \tag{2}$$

where ρ is the fluid density, ϕ is porosity, P is pressure, ν_{e} is an effective viscosity. $\boldsymbol{F}$ represents the total body force due to the presence of the porous medium and other external force fields, expressed by

$$\boldsymbol{F} = -\frac{\phi\nu}{K}\boldsymbol{v} - \frac{\phi F_\phi}{\sqrt{K}}|\boldsymbol{v}|\boldsymbol{v} + \phi G, \tag{3}$$

where ν is the shear viscosity of the fluid, which is generally different from ν_{e}. G is the body force induced by an external force, F_ϕ and K are respectively the geometric function and permeability, which are based on Ergun's experimental investigation,[13] and is expressed by Vafai as follows:[14]

$$F_\phi = \frac{1.75}{\sqrt{150\phi^3}}, \tag{4}$$

$$K = \frac{\phi^3 d_{\mathrm{p}}^2}{150(1-\phi)^2}, \tag{5}$$

with ϕ the porosity, and d_{p} the solid particle diameter.

Equations (1)–(5) are well established for single-phase flows but not suitable for MPFs in porous media. According to Ref.[15], for a MPF in a porous medium, relative permeability and surface tension should be taken into account in dynamic laws. In this paper, we consider only the case of two immiscible phases. This is just for simplicity, and for a general case one can obtain a similar conclusion as given below. The Darcy law for multi-phase $\boldsymbol{v}_\alpha = \sum_\beta K_{\alpha\beta}(\theta)\frac{K}{\mu_\alpha}\boldsymbol{X}_\beta$ ($\boldsymbol{X}_\beta$ is the body force acting on the βth component, $K_{\alpha\beta}(\theta)$ is the relative permeability coefficient, depending only on the saturation θ) is commonly concerned with three problems: 1) What is the domain of validity of the linearity between flux and body force? 2) The dependence of the permeability coefficients on the change of microgeometry is of considerable interest. 3) Any symmetry properties of the matrix $K_{\alpha\beta}$ are of considerable interest from the theoretical standpoint. These phenomenological descriptions form the theory of linear nonequilibrium thermodynamics. Based on the reversibility of the microscopic dynamics of atomic motion, Onsager first described the general theory of such processes with the reciprocity relations $K_{12} = K_{21}$,[6] and it was recently demonstrated by Flekkøy and Pride.[16] Through a careful analysis as in Refs.[5, 16, 17], we modify Eqs.(1)–(3) for the two-phase flows as

$$\nabla \cdot \boldsymbol{v}_\alpha = 0, \tag{6}$$

$$\frac{\partial \boldsymbol{v}_\alpha}{\partial t} + (\boldsymbol{v}_\alpha \cdot \nabla)\left(\frac{\boldsymbol{v}_\alpha}{\phi}\right) = -\frac{1}{\rho_\alpha}\nabla(\phi P) + \nu_{\mathrm{e}_\alpha}\nabla^2 \boldsymbol{v}_\alpha + \boldsymbol{F}_\alpha, \tag{7}$$

where the total force acting on fluid particles in the α phase is modified by adding the relative permeability and surface tension as follows,

$$\begin{aligned}\boldsymbol{F}_\alpha = &-\frac{\phi}{K}\left[\frac{\nu_\alpha}{K_{\alpha\alpha}(\theta)}\boldsymbol{v}_\alpha + \frac{\nu_\beta}{K_{\alpha\beta}(\theta)}\boldsymbol{v}_\beta\right] \\ &-\frac{\phi F_\phi}{\sqrt{K}}\left[\frac{1}{\sqrt{K_{\alpha\alpha}(\theta)}}|\boldsymbol{v}_\alpha|\boldsymbol{v}_\alpha \right. \\ &\left. + \frac{1}{\sqrt{K_{\alpha\beta}(\theta)}}|\boldsymbol{v}_\beta|\boldsymbol{v}_\beta\right] \\ &+ \phi[G_\alpha + G_\beta] + F'_\alpha, \\ &\alpha, \beta = 1, 2, \alpha \neq \beta.\end{aligned} \tag{8}$$

In Eq.(8), the coefficients $K_{\alpha\beta}$ ($\alpha, \beta = 1, 2$) are dimensionless relative permeability coefficients. The F'_α is

surface tension, which can be modelled by using Shan and Chen's method[17] and expressed as

$$\boldsymbol{F}' = -\nabla \Phi, \tag{9}$$

where Φ is a potential function representing fluid–fluid interaction, its explicit form is given as follows:

$$\Phi = G_{\sigma\overline{\sigma}}(\boldsymbol{x}, \boldsymbol{x}')\psi^{\sigma}(\boldsymbol{x})\psi^{\overline{\sigma}}(\boldsymbol{x}'), \tag{10}$$

where $G_{\sigma\overline{\sigma}}(\boldsymbol{x}, \boldsymbol{x}')$ is a Green function. For more details on the Eq.(10) and connection to multiple phase flows see Ref.[17].

To obtain the solution of Eqs.(6)–(10) is not easy because the geometries of porous media are usually complicated. Thanks to lattice Boltzmann computational techniques, important progress has been made for the study of fluid flows in porous media.[3,4] Some authors have set up a LBM for multi-phase systems using colour particles.[18] However, as pointed out by Chen and Doolen,[19] these LBM schemes have two shortcomings. First, the procedure of redistribution of the coloured density at each site requires a time-consuming calculation on local maxima; second, the perturbation step with the redistribution of coloured distribution function causes an anisotropic surface tension that induces unphysical vortices near interfaces. The second point is crucial since the procedure adopted is more or less artificial. In this paper, we consider the drag effects of the medium and present the multi-phase LBM equation in the form of statistical average

$$\begin{aligned} &\bar{f}^i_\alpha(\boldsymbol{x} + \boldsymbol{e}^i_\alpha \delta_t, t + \delta_t) \\ =&\bar{f}^i_\alpha(\boldsymbol{x}, t) - \frac{\bar{f}^i_\alpha(\boldsymbol{x}, t) - \bar{f}^{ieq}_\alpha(\boldsymbol{x}, t)}{\tau_\alpha} + F^i_\alpha \delta_t, \\ &\alpha = 1, 2, \end{aligned} \tag{11}$$

where δ_t is the time increment, $\bar{f}^i_\alpha(\boldsymbol{x}, t)$ and $\bar{f}^{ieq}_\alpha(\boldsymbol{x}, t)$ are respectively the volume-averaged distribution function and the equilibrium distribution function of αth phase at the representative elementary volume scale (in the following, the overbars will be omitted for the sake of convenience), τ_α is the relaxation time, F^i_α is the force for ith particle of αth phase. In the D2Q9 model[20] the discrete velocities are given by:

$$\boldsymbol{e}^i_\alpha = \begin{cases} 0, & \text{for } i = 0; \\ \left(\cos\dfrac{(i-1)\pi}{2}, \sin\dfrac{(i-1)\pi}{2}\right), & \text{for } i = 1-4; \\ \sqrt{2}\left(\cos\left[\dfrac{(i-5)\pi}{2} + \dfrac{\pi}{4}\right], \sin\left[\dfrac{(i-5)\pi}{2} + \dfrac{\pi}{4}\right]\right), & \text{for } i = 5-8. \end{cases} \tag{12}$$

The equilibrium distribution function is:

$$\begin{aligned} f^{ieq}_\alpha =& A^i \rho_\alpha \left[1 + \frac{\boldsymbol{e}^i_\alpha \cdot \boldsymbol{v}_\alpha}{RT} \right. \\ &\left. + \frac{(\boldsymbol{e}^i_\alpha \cdot \boldsymbol{v}_\alpha)(\boldsymbol{e}^i_\alpha \cdot \boldsymbol{v}_\alpha)}{2\phi(RT)^2} - \frac{\boldsymbol{v}_\alpha \boldsymbol{v}_\alpha}{2\phi RT}\right], \end{aligned} \tag{13}$$

where R is the gas constant, T the temperature of the fluid. The corresponding weight coefficients are $A^0 = 4/9, A^i = 1/9 (i = 1,2,3,4), A^i = 1/36 (i = 5,6,7,8)$. Based on Refs.[3, 4], we obtain

$$\begin{aligned} F^i_\alpha =& A^i \rho_\alpha \left(1 - \frac{1}{2\tau_\alpha}\right)\left(\frac{\boldsymbol{e}^i_\alpha \cdot \boldsymbol{F}_\alpha}{RT} \right. \\ &\left. + \frac{(\boldsymbol{e}^i_\alpha \cdot \boldsymbol{v}_\alpha)(\boldsymbol{e}^i_\alpha \cdot \boldsymbol{F}_\alpha)}{\phi R^2 T^2} - \frac{\boldsymbol{v}_\alpha \cdot \boldsymbol{F}_\alpha}{\phi RT}\right). \end{aligned} \tag{14}$$

The density and velocity of the fluid are defined as

$$\rho_\alpha = \sum_i f^i_\alpha, \qquad \boldsymbol{v}_\alpha = \sum_i f^i_\alpha \boldsymbol{e}^i_\alpha / \rho_\alpha + \frac{\delta_t}{2}\boldsymbol{F}_\alpha. \tag{15}$$

To recover macroscopic equations for αth phase flows in the porous medium, we use the multi-scale expansion

$$f^i_\alpha = f^i_{\alpha 0} + \epsilon f^i_{\alpha 1} + \epsilon^2 f^i_{\alpha 2} + O(\epsilon^3), \tag{16}$$

$$\boldsymbol{F}^\alpha = \epsilon \boldsymbol{F}^\alpha_1 + O(\epsilon^2), \tag{17}$$

$$\frac{\partial}{\partial t} = \epsilon \frac{\partial}{\partial t_1} + \epsilon^2 \frac{\partial}{\partial t_2} + O(\epsilon^3), \tag{18}$$

$$\frac{\partial}{\partial x} = \epsilon \frac{\partial}{\partial x_1} + O(\epsilon^2). \tag{19}$$

Letting $f^{\alpha 0}_i = f^{\alpha eq}_i$ and ignoring the terms of $O(\epsilon^3)$, we obtain

$$\frac{\partial \rho^\alpha}{\partial t} + \nabla \cdot (\rho^\alpha \boldsymbol{v}^\alpha) = 0, \tag{20}$$

$$\begin{aligned} &\frac{\partial(\rho^\alpha \boldsymbol{v}^\alpha)}{\partial t} + \nabla \cdot \left(\frac{\rho^\alpha \boldsymbol{v}^\alpha \boldsymbol{v}^\alpha}{\phi}\right) \\ =& -\nabla P + \nabla \cdot [\rho^\alpha \nu^\alpha_{\mathrm{e}} (\nabla \boldsymbol{v}^\alpha + \boldsymbol{v}^\alpha \nabla)] + \boldsymbol{F}^\alpha, \end{aligned} \tag{21}$$

where $\nu^\alpha_{\mathrm{e}} = (\tau - 0.5) RT \delta_t$. Note that when $\phi = 1$, Eq.(21) reduces to the standard lattice Boltzmann equation for the αth phase flow in the absence of the

porous medium. Another interesting character is that Eq.(21) is reduced to Darcy's law[20] when the αth phase flow in the porous medium is very slow.

3. The interfacial boundary conditions

The interfacial boundary conditions are extremely important for obtaining an accurate result for the numerical simulation. In the fluid-solid interfacial regions, bouncing-back boundary condition[21] is a primary method in the lattice-Boltzmann simulation and has been proven to have first-order accuracy. More accurate boundary conditions have been proposed in the past few years.[22] In this paper we use the scheme for the treatment of the boundary condition by considering a curved boundary lying between the nodes of the equidistant lattice of space $\Delta\delta x$ for a two-dimensional model, as shown in Fig.1.

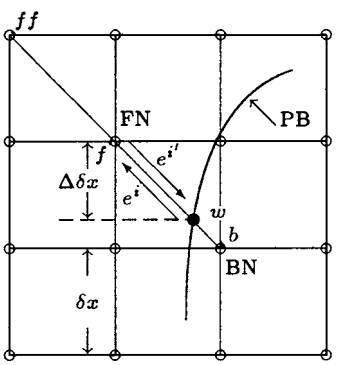

Fig.1. Layout of the regularly spaced lattice and curved wall boundary, BN represents boundary node, PB represents physical boundary, and FN represents fluid node.

The lattice nodes on the solid and fluid sides are denoted by $\boldsymbol{x}_b$ and $\boldsymbol{x}_f$ respectively. We assume $\boldsymbol{e}^i = \boldsymbol{x}_b - \boldsymbol{x}_f$ and $\boldsymbol{e}^{i'} = -\boldsymbol{e}^i$. The filled small circle at $\boldsymbol{x}_w$ is the intersection of the physical boundary with the link between $\boldsymbol{x}_b$ and $\boldsymbol{x}_f$. The fraction of an intersected link in the fluid is Θ, defined as

$$\Theta = \frac{|\boldsymbol{x}_f - \boldsymbol{x}_w|}{|\boldsymbol{x}_f - \boldsymbol{x}_b|}, \qquad 0 \le \Theta \le 1. \tag{22}$$

After a collision step, the distribution functions at $\boldsymbol{x}_f$ and t are known as the following streaming step

$$f^i(\boldsymbol{x}_f, t + \delta t) = f^i(\boldsymbol{x}_{ff}, t), \tag{23}$$

while $f^{i'}(\boldsymbol{x}_f)$ can be obtained by

$$f^{i'}(\boldsymbol{x}_f, t + \delta t) = f^{i'}(\boldsymbol{x}_b, t). \tag{24}$$

However, the distribution function $f^{i'}(\boldsymbol{x}_b, t)$ at the boundary node is unknown. According to Ref. [22], we assume that $f^{i'}(\boldsymbol{x}_b, t)$ satisfies the following linear interpolation formula

$$f^{i'}(\boldsymbol{x}_b, t) = (1-\chi) f^i(\boldsymbol{x}_f, t) + \chi f^{i^*}(\boldsymbol{x}_b, t) + 6\alpha_i \boldsymbol{e}^{i'} \cdot \boldsymbol{v}_w, \tag{25}$$

where $\boldsymbol{v}_w = \boldsymbol{v}(\boldsymbol{x}_w, t)$ is the velocity at the physical boundary and χ is a parameter. f^{i^*} is a fictitious equilibrium distribution function given by

$$f^{i^*}(\boldsymbol{x}_b, t) = t_{\mathrm{p}}\rho\left\{1 + \boldsymbol{e}^{i\alpha} \cdot \boldsymbol{v}_{\alpha bf} + \frac{\boldsymbol{v}_{\alpha f} \cdot \boldsymbol{v}_{\beta f}}{2}(\boldsymbol{e}^{i\alpha} \cdot \boldsymbol{e}^{i\beta} - \delta_{\alpha\beta})\right\}, \tag{26}$$

where $\boldsymbol{v}_{\alpha f} = \boldsymbol{v}_\alpha(\boldsymbol{x}_b, t)$ and $\boldsymbol{v}_{\beta f} = \boldsymbol{v}_\beta(\boldsymbol{x}_b, t)$ are the fluid velocities near the solid and $\boldsymbol{v}_{bf}$. In Ref.[23], Fillipova and Hanel proposed

$$\boldsymbol{v}_{bf} = (\Theta - 1)\boldsymbol{v}_f/\Theta + \boldsymbol{v}_w/\Theta;$$

$$\chi = (2\Theta - 1)/\tau \qquad \text{for} \qquad \Theta \ge \frac{1}{2}, \tag{27}$$

and

$$\boldsymbol{v}_{bf} = \boldsymbol{v}_f;$$

$$\chi = (2\Theta - 1)/(\tau - 1) \qquad \text{for} \qquad \Theta \le \frac{1}{2}, \tag{28}$$

to obtain a second-order scheme for the "slow flow". Mei *et al*[24] improved the stability of the scheme by replacing Eq.(27) by

$$\boldsymbol{v}_{bf} = \boldsymbol{v}_{ff};$$

$$\chi = (2\Theta - 1)/(\tau - 2) \qquad \text{for} \qquad \Theta \le \frac{1}{2}. \tag{29}$$

They have used this improved technique to study several flow problems such as the fully developed flow in a square duct, lid-driven cavity flows, fully developed flows inside a circular pipe and a uniform flow over a sphere to demonstrate its accuracy and robustness.

Periodic boundary conditions are chosen, and so it is ensured that escaping particles at the end of the flow domain can be reintroduced at its beginning.

4. Example

As a test of this method, we simulate the separation in the case of two immiscible fluids. Potentially, one of the most commercially rewarding applications of such a case is its use in enhanced oil recovery. In oil field flows, oil is displaced and carried to the surface by water. We perform simulations so as to reproduce such oil field extraction flows. To the whole two-phase system, the total density ρ satisfies:

$$\rho = \rho_1 + \rho_2, \tag{30}$$

and the local velocity must satisfy

$$\rho \boldsymbol{v} = \sum_{\alpha,i} f_\alpha^i \boldsymbol{e}_\alpha^i = \sum_{\alpha,i} f_{\alpha eq}^i \boldsymbol{e}_\alpha^i. \tag{31}$$

To demonstrate the application of our model, we take a square two-phase fluid domain with the sides of length L and divide it into 512×512 lattice. The initial density of the 1st phase at every site is randomly produced between 0.5 and 0.55, while the 2nd phase is determined by the condition: $\rho_1 + \rho_2 = 1$. Other parameters are chosen to be $\phi = 0.1$, $K = 5 \times 10^{-14}\mathrm{m}^2$, $\nu_e = 1 \times 10^{-3}\mathrm{kgm}^{-1}s^{-1}$, and $\lambda_f = 0.105$.

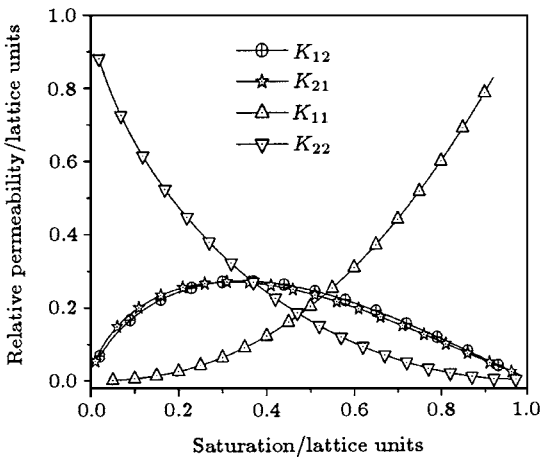

Fig.2. Relative permeability corresponding to our model.

Figure 2 shows that the relative permeability coefficients agree well with the theoretical prediction. The two coupling coefficients K_{12} and K_{21} have the same magnitude, so the linear flux-force relationships satisfy the Onsager reciprocity. Thus we may conclude that our model is reliable.

Figure 3 illustrates the separation of the two-phase fluid in porous media. Phase separation phenomenon is shown with the time evolution of density distribution. For all pictures in Fig.3, the white regions represent one phase, black ones represent the other phase, and grey points that are in both white regions and black regions, generated by the smoothing of random white-noise images,[25] represent solid media. All the results are in complete agreement with those numerical results obtained in two dimensions by Maillet and Coveney[26,27] and experimental results.[28] At the same time, the dynamical rules of our model are local, so it is more physical and can be run on massively parallel computers with well computational efficiency.

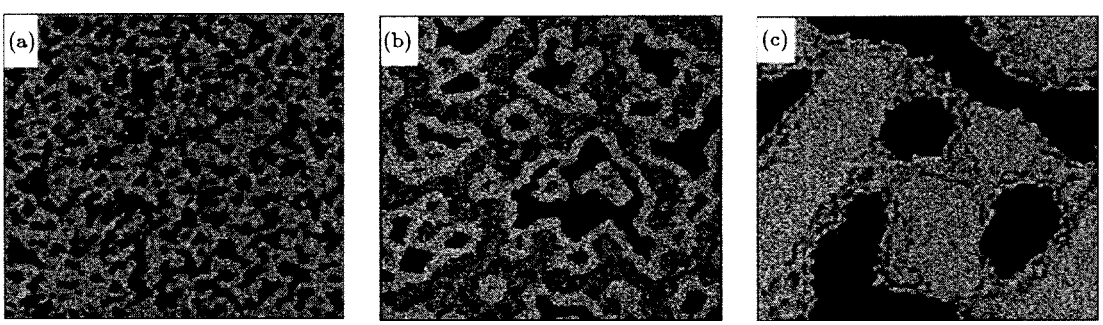

Fig.3. Separation of a two-phase fluid in porous media on a 512×512 lattice. Shown are the time evolutions of the density distribution at (a) $t = 10$, (b) $t = 900$, (c) $t = 5600$.

5. Conclusion

A new LBM scheme has been extended to simulate the multiphase flow in porous media. The description of macroscopic behaviour of two-immiscible-fluid flows by modifying the Navier-Stokes equations of Nithiarasu *et al* with an explicit viscous coupling between species has been verified. In the test, the dependence of the relative permeability for the forced fluid bears a strong similarity to the results obtained from other numerical models and flows in sands. The two cross coupling coefficients K_{12} and K_{21} have the statistical magnitude of the LBM. This linear flux-force relationship satisfies the Onsager reciprocity, as expected. Such a study could elucidate which behaviours for the separation of multiphase fluids are due to the modification of Navier-Stokes equations and which are due to other factors, such as modification of the interfacial boundary conditions.

Acknowledgment

The authors would like to thank Dr Haiping Fang for his help.

References

[1] Family F and Vicsek T 1991 *Dynamics of Fractal Surfaces* (Singapore: World Scientific)
[2] Martys N S and Chen H D 1996 *Phys. Rev.* E **53** 743
[3] Kang Q J, Zhang D X and Chen S Y 2002 *Phys. Rev.* E **66** 6307
[4] Guo Z L and Zhao T S 2002 *Phys. Rev.* E **66** 6304
[5] Nithiarasu P, Seetharamu K N and Sundararajan T 1997 *Int. J. Heat Mass Transfer.* **40** 3955
[6] Cancelliere A *et al* 1990 *Phys. Fluids* A **2** 2085
[7] Vedvik A *et al* 1998 *Phys. Rev. Lett.* **80** 3065
[8] Olson J F and Rothman D H 1997 *J. Fluid Mech.* **341** 343
[9] Ziegle O P 1993 *J. Stat. Phys.* **71** 1171
[10] Batchelor G K 1967 *An Introduction to Fluid Dynamics* (UK, Cambridge: Cambridge University Press)
[11] Rothman D H and Zaleski S 1994 *Rev. Mod. Phys.* **66** 1417
[12] Xu Y S and Xu X Z 2002 *Chin. Phys.* **11** 583
[13] Ergun S 1952 *Chem. Engng.* Pro **48** 89
[14] Vafai K 1984 *J Fluid Mech.* **147** 233
[15] Bear J 1972 *Dynamics of Fluids in Porous Media* (New York: Dover)
[16] Flekkøy E G and Pride S R 1999 *Phys. Rev.* E **60** 4130
[17] Shan X W and Chen H D 1993 *Phys. Rev.* E **47** 1845
[18] Gunstensen A K *et al* 1991 *Phys. Rev.* A **43** 4320
[19] Chen S Y and Doolen G D 1998 *Ann. Rev. Fluid Mech.* **30** 329
[20] Qian Y H, d'Humiéres D and Lallemand P 1992 *Europhys Lett.* **17** 479
[21] Noble *et al* D R 1995 *Phys. Fluids.* **7** 203
[22] Fang H P, Wan R Z and Fan L W 2000 *Chin. Phys.* **7** 515
[23] Filippova O and Hanel D 1997 *Comput. Fluids.* **26** 697
[24] Mei R W, Luo L S and Shyy W 1999 *J. Comput. Phys.* **155** 307
[25] Schwartz L M and Banavar J R 1989 *Phys. Rev.* B **39** 965
[26] Mailllet J B and Coveney P R 2000 *Phys. Rev.* E **62** 2898
[27] Love P J, Mailllet J B and Coveney P V 2001 *Phys. Rev.* E **64** 1302
[28] Wyckoff R D and Botset H G 1936 *Physics* **7** 325